nature portfolio

Peer Review File

Spatial metabolic gradients in the liver and small intestine

Corresponding Author: Professor Joshua Rabinowitz

Any redactions in this file are there to maintain patient confidentiality, the confidentiality of unpublished data, or to remove third-party material.

This file contains all reviewer reports in order by version, followed by all author rebuttals in order by version.

Reviewer 3 was not able to participate in the final round of review. Their expertise was covered by Reviewers #1 and #2. The final version of this manuscript file has passed peer review.

Version 0:

Reviewer comments:

Referee #1

(Remarks to the Author)
In this study, the authors characterize the spatial gradients of the abundance of over 100 metabolites in the murine liver and small intestine by primarily leveraging MALDI imaging mass spectrometry, isotope tracing, and computational methods, particularly an adaptation of the GASTON deep learning method. Briefly, this method learns one or multiple scalars that encode information about the abundance of different metabolites in space. The authors demonstrate that these scalars, referred to as metabolic depths, recapture the major axes of metabolite gradients in the murine liver, namely the portal-to-central vein axis, and in the small intestine, i.e. the crypt-to-tip axis and the border-to-basal membrane. Along these axes, the authors analyze the changes in the abundance of metabolites, identifying, for example, mitochondria-rich areas in both the murine liver and intestine as zones having a high and partially unsatisfied energy demand. Exploring the metabolism of fructose in greater detail, the authors describe that fructose is usually metabolized through a combination of the periportal regions in both the liver and small intestine. However, for large doses, they observe a spill-over effect to the pericentral liver, where the partial metabolism of fructose induces energy stress. While the analysis focuses on the murine liver and small intestine, the leveraged experimental and computational methods appear to be easily transferable to the study of other organs and species. The story is a very well written and a welcome addition to the field, which is mostly featuring RNA- and protein-based spatial profiling. However, some points should be addressed before publication as detailed below.

Major points:

1. While some findings are novel and surprising (e.g. ATP/AMP ratio in the liver), this paper mostly adds metabolite data fitting with spatially confined metabolic processes which have been identified/described previously using other methods – therefore adding limited novel biology data (at least for the liver part, I am not familiar with gut metabolism literature). I therefore mostly see this paper as a technology and resource paper. However, the deep learning method seems to be submitted elsewhere. For a resource paper, the authors should add a user-friendly shiny app making their data available and thereby increasing the impact of this work.

2. According to the authors, they selected the specific hyperparameters for the MET-MAP model because these configurations showed the “lowest loss and efficient training times.” The authors should consider adding a detailed description in the supplemental material of the different configurations they tested and the respective loss curves and training time estimates eventually guiding their selection.

3. I very much appreciate that the authors made their code to run the analysis publicly available. However, the repository (https://github.com/raphael-group/Multi-GASTON) currently lacks detailed instructions on how to setup the environment to run the code and how to use it to reproduce the results in the paper. The authors should add such information to facilitate its use and promote the reproducibility of their study.

4. The authors show interesting data around fructose-induced focal metabolic derangements, which could possibly help to understand the developed of MASH. Unless this is considered a pure resource paper, the authors should expand this angle significantly and validate potential new hypothesis in vivo using modulators (e.g. small molecules, siRNAs) to modulate metabolic activity.

Minor comments:

5. Several sections of the Methods section in the paper provide only rough estimates with respect to the parameters used in the computational analysis. For example, they report the number of selected hidden nodes as "300-400" (line 611), the number of metabolites used as input as "about 100," the metabolic depths to be excluded as having "close-to-zero weights" (line 645), and the size of the cropped regions as "n x n" (line 714). The authors should provide specific details to ensure the reproducibility of the study.

6. The authors mention that K=4 was used when the correct choice of K was unclear. However, it appears that K=4 was not used for any of the analyses. Instead, K=1 (line 588) was used for the analysis of the murine liver data, and K=3 (line 651) was used for the analysis of the murine intestine data. The authors then further refer to "one or two" significant metabolic depths that were identified depending on the individual sample quality and resolution (line 652-653). Presumably, these are the ones for which the corresponding weights of the depth functions were not "close-to-zero" In the spirit of my last comment, the authors should rephrase the text to clarify this and indicate the specific choices of K for each analysis they conducted.

7. This is just a question out of interest to which I would appreciate an answer – there is no need to address this during the revisions: the authors introduce an adaptation of the GASTON model, which they refer to as MET-MAP. At a high level, the model takes the positional coordinates as input and predicts the abundance of different metabolites at the corresponding spatial locations. To achieve this, a one-hidden-layer neural network first outputs K scalars, referred to as metabolic depths, which are then input to a second neural network. This second network may either include another hidden layer (for the liver) or consist of just a single layer (for the intestine) to predict the metabolite abundances. Given that the authors find almost all metabolites to show spatial gradients and many of them appear to be monotonically increasing or decreasing along the major metabolic axes, I am wondering if a non-linear PCA implemented by e.g. a simple autoencoder model could also provide similar estimates of those of the metabolic depth.

(Remarks on code availability)
Code for the MET-MAP Model (https://github.com/raphael-group/Multi-GASTON):
The code itself is well-structured, easy to understand, and nicely commented. Unfortunately, the README file still seems incomplete, as the installation instructions, for example, are missing. Additionally, the file lacks a detailed description of how to reproduce the results of the study. However, given that the repository is intended as a resource for another Methods paper, I propose creating a separate GitHub repository that provides the minimal code required to reproduce the results of the study under review (see the last paragraph).

Code for the supervised vein detection (https://github.com/xxing9703/Liver_vein_detection/tree/main):
While the README file of this repository contains a high-level description of the main components of the implemented pipeline for identifying portal and central veins from MALDI images, it would significantly benefit from the following changes to enhance the usability of the code. First, the README is incomplete; for example, in the section describing the script "--script_get_imax.m", the reference for where to download example images is missing. Second, the code itself should include docstring comments to consistently describe the input and output of the individual functions, as well as a few inline comments to improve its reusability. In this context, restructuring the code to group functions into larger modules and consolidating these into a single MATLAB file, instead of having separate files for each function, would also be beneficial.

Reproducing the study results:
As mentioned before, the referenced repository used in the course of the study currently lacks sufficient details on how to reproduce the study results with the referenced data in https://doi.org/10.6084/m9.figshare.28049555.v3. Since the individual packages might be reused, or, in the case of Multi-Gaston, tailored towards more general use-cases, I recommend creating a new GitHub repository to outline how to reproduce the results of the study by, among other things, using the repositories commented on above. I understand that this might be a time-consuming task, but it would greatly improve the reproducibility of the study and demonstrate how to apply the individual packages, thus promoting their reusability for other researchers in their own studies.

I would finally like to reiterate that I very much appreciate that the authors made their code and data publicly available on platforms adhering to the FAIR principles.

Referee #2

(Remarks to the Author)
Samarah et al. used MALDI-based mass spectrometry imaging to assess metabolite localization in two organs from mice: liver and intestine. They develop a computational workflow to report metabolite gradients in both organs, focusing on periportal-pericentral gradients in the hepatic lobule, and crypt-tip gradients in the intestinal villus. They find that the great majority of detectable metabolites display localized gradients. Some of these gradients could be predicted from existing gene expression studies, but others (e.g. counterintuitive AMP/ATP gradients in the liver; F1P gradients in the liver after fructose feeding) identify interesting new aspects of nutrition and metabolism. The authors also use stable isotope-labeled nutrients to assess regional metabolic activity, and this adds another important dimension to this detailed characterization of metabolic localization within organs. I suggest that the paper be clarified or strengthened in a few areas:

1. Given the untargeted nature of MSI, it is surprising that only 170 ions were “reliably detected.” I assume this means that these were reproducibly detected in independent samples, and molecular assignments could be made with high confidence based on standards? This seems to be what the Methods section implies, but this should be clarified in a sentence or two in the main text.
2. In Fig. 1f, how is the PN-to-CV normalized distance calculated? The absolute distance from portal to central varies among individual lobules, and likely with whether the slice through the lobule was axial or diagonal.
3. In Fig. 2a, what are the “unclassified” metabolites? If these are unannotated masses, could their spatial correlation with other metabolites assist in identifying them?
4. In the isotope tracing experiments, did the authors acquire data on all isotopologues in the metabolites of interest? If so, this could add specificity and clarity to their interpretation of the labeling patterns. For example, it is surprising in the 13C-lactate infusions (Fig. 5b) that m+2 labeling seems to exceed m+3 labeling, at all locations, and that the m+3/m+2 labeling ratio is always far less than 1.0. This seems to argue against the notion that carbon entry via PC exceeds entry via PDH in the liver.
5. The authors nicely show that lactate contributes more to glutamate in well-oxygenated crypts, and glutamine is a more meaningful carbon source in the tips. This implies that different carbon sources are catabolized differently along the villus. But I am still confused as to why citrate is more abundant in the crypts, while other TCA cycle intermediates are relatively depleted. Is there a change in aconitase/IDH expression between crypt and tip?
Minor:
1. In Fig. 2a, consider changing the color scheme to make it easier to differentiate the pentose phosphate pathway intermediates (accumulated in periportal region) from the phospholipids (accumulated in the pericentral region).

(Remarks on code availability)
I did not review the AI/deep learning code, as I do not think I would be able to interpret it. However the basic statistical analyses they use for localization gradients seem appropriate.

Referee #3

(Remarks to the Author)
In this work, Samarah et al perform comprehensive spatial metabolomics of the major metabolic organs – the small intestine and the liver, in mice. These tissues are highly structured and exhibit strong gradients of oxygen, nutrients and morphogens. As a result, both mRNA and protein levels for most genes have been shown to strongly vary along the axes of the repeating units of these tissues, lobules in the liver and crypt-villi units in the intestine. However, obtaining high-spatial resolution spatial maps of the metabolites has been challenging, in part due to the lower sensitivity of spatial approaches for measuring metabolites, such as MALDI. The authors overcome this limitation with a sophisticated AI-driven approach that enables annotating individual pixels to the major tissue coordinates. They then pool many pixels from similar zones, thus increasing signal to noise ratio and sensitivity, yielding a highly detailed map of more than a hundred metabolites. They use the results to obtain interesting insights regarding energy and metabolite utilization. Importantly, they perform the mapping on both a fasted ‘steady state’, as well as after refeeding fasted mice with labeled fructose and glucose, enabling spatial mapping of the metabolic fluxes associated with the absorption of these central nutrients. The paper is both an important resource and a methodological breakthrough, since the approaches presented can be readily generalized to enable attaining similar spatial metabolic maps in other structured tissues, as well as in tumors.
I have a few comments that should be addressed in a revision:
1) Some metabolites are labile, and their measurements could potentially be skewed by factors such as temporal delays in tissue processing for MALDI, as well as by features of the technique, such as matrix effects. The study focuses on relative changes along the axes of the tissues, so such effects may be less critical, however, it would strengthen the paper to add a controlled measurement using an orthogonal approach. For example, LC-MS bulk measurements of several metabolites, demonstrating the the relative proportions between them are quantitatively similar to those observed with the MALDI measurements.
2) Line 175-176 – Liver energetic demands are also high because of protein translation. The periportal zone is the main site of translation of secreted proteins (such as albumin, complement and clotting factors), I would mention this task as well.
3) Line 221 – Cholesterol absorption from the lumen is strongly zonated towards the villus tip (e.g. both the mRNA and proteins of NPC1L1, https://www.cell.com/cell/fulltext/S0092-8674(18)31164-4 and Harnik et al.). Might this also contribute to the tip zonation of Cholesterol sulfate?
4) One of the most prominent zonated programs at the mouse villus tip is the expression of the purine metabolism enzymes Enpp3, Nt5e (CD73), Slc28a2 and Ada, which convert ATP (presumably from luminal bacteria) to AMP, then to Adenosine and finally to inosine (https://www.cell.com/cell/fulltext/S0092-8674(18)31164-4). Can this program in tip enterocytes affect some of the observed gradients in ATP and AMP?
5) KHK protein peaks at the middle of the villus rather than at the villus tip as mentioned in EDF6f caption. It is different than most transporters and nutrient-processing enzymes, the protein expression of which peaks at the villus tip. This could potentially explain the stronger absorption the authors measure for fructose at the mid/bottom villus shortly after the gavage. I would change the legend of EDF6f to reflect the mid-villus localization of KHK.
6) One of the riddles in liver biology is the glucose paradox (Katz and McGarry, 1984), positing that the main substrate of glycogen synthesis in the liver after a meal is lactate, via the indirect pathway, rather than glucose. Moreover, it was postulated that this indirect lactate utilization is specifically applied in the portal zones (Figure 3 in doi: 10.1146/annurev.nu.16.070196.001143). Can the results of the labeled fructose+glucose refeeding experiment be used to assess this potential differential usage of lactate vs. glucose as a substrate for glycogen replenishment postprandially?
7) Line 556 – MALDI-IMS data processing – Should the MALDI signal be normalized to the summed signal of all measured metabolites before averaging over pixels of same zone to obtain the zonation profiles? If different pixels have different total

metabolite yield (metabolite capture rates), such normalization could potentially control for this extrinsic source of variability.

(Remarks on code availability)

Version 1:

Reviewer comments:

Referee #1

(Remarks to the Author)
I thank the authors for addressing all my points. Great work.

(Remarks on code availability)
My expert data scientist reviewed the code in the original and the revised manuscript. His comments aiming at allowing reproducibility, proving readme file etc have all been addressed by the authors.

Referee #2

(Remarks to the Author)
The revision address my critiques and I believe the paper should be published.

(Remarks on code availability)

Open Access This Peer Review File is licensed under a Creative Commons Attribution 4.0 International License, which permits use, sharing, adaptation, distribution and reproduction in any medium or format, as long as you give appropriate credit to the original author(s) and the source, provide a link to the Creative Commons license, and indicate if changes were made.
In cases where reviewers are anonymous, credit should be given to 'Anonymous Referee' and the source.
The images or other third party material in this Peer Review File are included in the article's Creative Commons license, unless indicated otherwise in a credit line to the material. If material is not included in the article's Creative Commons license and your intended use is not permitted by statutory regulation or exceeds the permitted use, you will need to obtain permission directly from the copyright holder.
To view a copy of this license, visit https://creativecommons.org/licenses/by/4.0/

Reviewer comments and responses

Manuscript: Spatial metabolic gradients in the liver and small intestine; Samarah *et al.*

Referee #1:

General comment: “In this study, the authors characterize the spatial gradients of the abundance of over 100 metabolites in the murine liver and small intestine by primarily leveraging MALDI imaging mass spectrometry, isotope tracing, and computational methods, particularly an adaptation of the GASTON deep learning method. Briefly, this method learns one or multiple scalars that encode information about the abundance of different metabolites in space. The authors demonstrate that these scalars, referred to as metabolic depths, recapture the major axes of metabolite gradients in the murine liver, namely the portal-to-central vein axis, and in the small intestine, i.e. the crypt-to-tip axis and the border-to-basal membrane. Along these axes, the authors analyze the changes in the abundance of metabolites, identifying, for example, mitochondria-rich areas in both the murine liver and intestine as zones having a high and partially unsatisfied energy demand. Exploring the metabolism of fructose in greater detail, the authors describe that fructose is usually metabolized through a combination of the periportal regions in both the liver and small intestine. However, for large doses, they observe a spill-over effect to the pericentral liver, where the partial metabolism of fructose induces energy stress. While the analysis focuses on the murine liver and small intestine, the leveraged experimental and computational methods appear to be easily transferable to the study of other organs and species. The story is a very well written and a welcome addition to the field, which is mostly featuring RNA- and protein-based spatial profiling. However, some points should be addressed before publication as detailed below.”

Response: We thank the reviewer for their feedback and suggestions to strengthen the paper.

1. “While some findings are novel and surprising (e.g. ATP/AMP ratio in the liver), this paper mostly adds metabolite data fitting with spatially confined metabolic processes which have been identified/described previously using other methods – therefore adding limited novel biology data (at least for the liver part, I am not familiar with gut metabolism literature). I therefore mostly see this paper as a technology and resource paper. However, the deep learning method seems to be submitted elsewhere. For a resource paper, the authors should add a user-friendly shiny app making their data available and thereby increasing the impact of this work.”

Response: We thank the reviewer for the recommendation. We have created “MET-MAP” (https://metmap.princeton.edu/), a user-friendly R-Shiny-based app that enables users to visualize the metabolic topography, metabolite ion images and spatial gradients in murine liver and small-intestine epithelium. Users have access to visualize our results from the spatial metabolomics data sets in both tissues. We included liver and small-intestine data across n = 8 and n = 7 mice, respectively.

MET-MAP app description:

“Metabolic Topography” tab: In this tab, the rectangular crops that were selected for analysis by MET-MAP are displayed over the full liver slice analyzed by MALDI-MSI (gray area). The metabolic topography is shown as a contour plot, with contour regions varying in color

depending on their respective metabolic depth. In addition, users can select to visualize images of the metabolic topography for the small-intestine epithelium.

"Metabolite images & gradients" tab: Here, users can select to view ion images for metabolites and lipids across liver slices. Spatial gradients quantified by MET-MAP can be visualized as a graph of mean ion count vs metabolic depth for crops outlined in red (same crops as in the "Metabolic Topography" tab). To exclude liver portal and central blood vessels from analysis, we recommend users to display spatial gradients at $0.05 \leq$ metabolic depth ≤ 0.95, which is the default range. Similarly, users can visualize ion images for selected metabolites and lipids in the intestinal epithelium and their corresponding spatial gradients. Note that the metabolites listed follow the same metabolite order in Supplementary Table 1 (for liver) and Supplementary Table 3 (intestine).

2. "According to the authors, they selected the specific hyperparameters for the MET-MAP model because these configurations showed the "lowest loss and efficient training times." The authors should consider adding a detailed description in the supplemental material of the different configurations they tested and the respective loss curves and training time estimates eventually guiding their selection."

Response: We thank the reviewer for the suggestion. We added two new sections in the Supplemental Information that provide detailed description of the hyperparameters for the MET-MAP models that were used for the liver and small intestine:

MET-MAP hyperparameters used in liver data analysis

Four batches of murine liver spatial metabolomics data were analyzed in this study: unperturbed, glutamine-tracer infusion, lactate-tracer infusion, and oral 13C-fructose gavage. For all groups, MET-MAP was applied to adjacent rectangular liver crops to: (1) use spatial coordinates as the input layer, (2) learn a metabolic depth function with a hidden layer with 400 nodes, mapping spatial coordinates to a one-dimensional latent space, (3) learn a metabolite abundance function with two hidden layers of 10 nodes each, mapping the 1-D latent space (metabolic depth) to predicted metabolite abundances, and (4) compute the loss by comparing these predictions with the measured abundances. In particular, we settled on this architecture for the two learned functions after evaluating smaller neural network architectures, from one hidden layer of 200 nodes for the metabolic depth function and one hidden layer of 10 nodes for the abundance function. The smaller model had large discrepancies between predicted and actual metabolite abundances. We gradually increased model complexity until training loss was low and the metabolic depth result clearly recovered the underlying blood vessel patterns. All four batches of liver data were trained for up to 12,000 epochs or until convergence, defined as when the change in training loss falls below 1×10^{-10}. Convergence occurred within 30 minutes of real time (Supplementary Figure 1B, also shown below).

Due to the non-convexity of the loss function, each liver crop was trained using 10 random initializations. The best trial was selected based on 1) the lowest training loss, which is the squared difference between measured and predicted metabolite abundances, and 2) visual assessment (Supplementary Figure 1, shown below). Specifically, visual assessment was important for samples containing local abnormalities, such as tissue tears or large blood vessels sliced longitudinally, or for those exhibiting strong edge-to-tissue interior gradients, typically stemming from sample preparation. In such cases, some initializations of MET-MAP could

converge to a local minimum solution aligned with the axis from the tissue edge to tissue interior. Since our focus was on portal-central gradients, we selected MET-MAP trials that achieved the lowest training loss while avoiding macroscopic gradients related to sample preparation (Supplementary Figure 1C, shown below). Liver crops in which all initializations showed primarily macroscopic gradients were excluded from further analysis (25% of all analyzed crops).

MET-MAP hyperparameters used in small-intestine epithelium analysis

Same as in murine liver, four batches of data were analyzed in murine small intestine: unperturbed, glutamine-tracer infusion, lactate-tracer infusion, and oral 13C-fructose gavage. For all groups, MET-MAP was applied to the epithelial pixels to learn (1) a metabolic depth function with two hidden layers of 120 nodes each, and (2) a linear abundance function with no hidden layer. Models were trained for up to 30,000 epochs or until convergence, with empirical runtimes under an hour.

A hyperparameter of K = 3 metabolic depths was used for all data batches. The choice of 3 metabolic depths aligns with 3 biologically relevant dimensions of spatial variation in the intestinal epithelium: villus crypt-tip, epithelium apical-basolateral, and intestine proximal-distal (the latter potentially also covering any macroscopic patterns arising from imperfect sample processing or analysis). When analyzing with a single metabolic depth, some specimens returned each of these 3 patterns, or hybrids thereof, whereas analysis using K = 3 metabolic depths typically yielded a depth cleanly reflecting the crypt-tip dimension of interest.

For each sample, a grid search over the Lasso coefficient λ ranging from 0.0001 to 0.01 was conducted, with 5 random initializations per coefficient. The best trial was selected based on the lowest abundance prediction loss (defined as training loss minus the Lasso penalty term), combined with visual assessment for crypt-tip gradients.

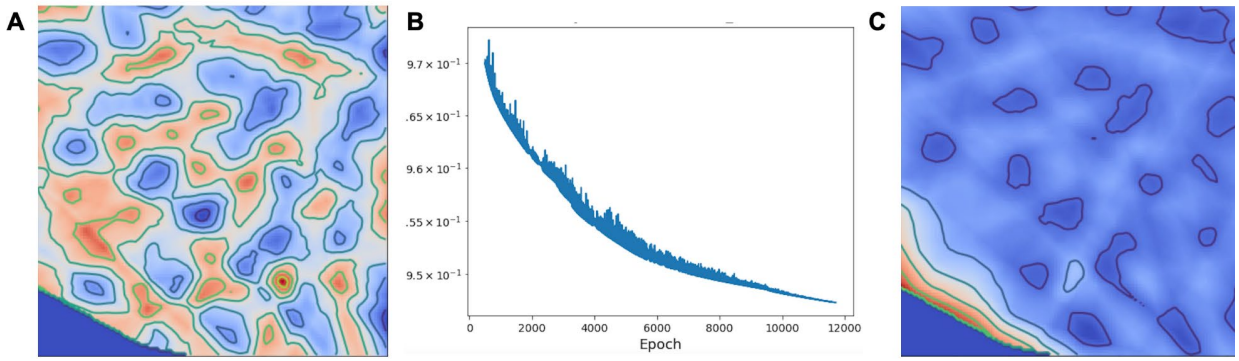

Supplementary Figure 1. (A) Metabolic depth from the best MET-MAP trial reveals the PN-CV axis on an example of a murine liver crop. (B) Training loss curve showing convergence within 12,000 epochs. (C) Metabolic depth from a different trial on the same liver crop, exhibiting tissue-edge to tissue-interior gradient.

3. “I very much appreciate that the authors made their code to run the analysis publicly available. However, the repository (https://github.com/raphael-group/Multi-GASTON)

currently lacks detailed instructions on how to setup the environment to run the code and how to use it to reproduce the results in the paper. The authors should add such information to facilitate its use and promote the reproducibility of their study."

We have created a new repository (https://github.com/raphael-group/MET-MAP) with tutorials containing detailed instructions on how to run MET-MAP to reproduce exemplary results for liver and intestine, which are included in the paper. The same deep-learning model parameters applied for the liver in the tutorial were used for all other liver samples, and the same applies for the small intestine.

4. "The authors show interesting data around fructose-induced focal metabolic derangements, which could possibly help to understand the developed of MASH. Unless this is considered a pure resource paper, the authors should expand this angle significantly and validate potential new hypothesis in vivo using modulators (e.g. small molecules, siRNAs) to modulate metabolic activity."

Response: We appreciate the reviewer's suggestion to follow up on our results from oral fructose in the liver. We agree that further experiments are merited. That said, the current "resource" version of the paper was well generally received and is a timely contribution. A more thorough treatment of MASH would likely require at least one year of additional work.

5. "Several sections of the Methods section in the paper provide only rough estimates with respect to the parameters used in the computational analysis. For example, they report the number of selected hidden nodes as "300-400" (line 611), the number of metabolites used as input as "about 100," the metabolic depths to be excluded as having "close-to-zero weights" (line 645), and the size of the cropped regions as "n x n" (line 714). The authors should provide specific details to ensure the reproducibility of the study."

Response: We added the specific details below to the Methods section.

On page 15, in the section "MALDI-IMS data processing", we specified the number of m/z peaks that were used in MET-MAP analysis: "Since this process does not filter out background signal (including MALDI matrix peaks) and isotopologues, we matched m/z peaks with metabolites measured in-house by LC-MS analysis of liver and intestine extracts within a mass window of ± 15 ppm and with metabolites in the Human Metabolome Database (HMDB, https://hmdb.ca/) and lipids from LIPID MAPS (https://www.lipidmaps.org/), yielding 156 matching m/z peaks in liver and 206 in intestine. Of the 156 m/z peaks in liver, 144 corresponded to deprotonated metabolites and lipids (the remaining 12 peaks comprised other ion adducts, e.g., $[M+Na-2H]^-$, $[M+K-2H]^-$, or $[M+Cl]^-$) (Supplementary Table 1). For the intestine, 176 ions corresponded to deprotonated metabolites and lipids, with the remaining 30 peaks as sodium, potassium, chloride adducts or dehydrated ($[M-H2O-H]^-$) (Supplementary Table 3). Ion intensities for the 156 metabolites and lipids in liver and the total ion count at each pixel were extracted and used for deep-learning analysis, whereas 206 metabolites and lipids were used for k-means clustering of the intestine data and subsequent analysis by MET-MAP.

On page 16, under **"Deep learning of liver metabolic topography",** we added the following sentence to specify the number of hidden layers and nodes in the neural network used for liver

data: “The hyperparameter K was chosen based on the number of distinct patterns expected in the data. For the liver, we expected portal-central gradient to be the predominant spatial axis. As such, we trained the metabolic depth function using a single hidden layer (K = 1) with 400 nodes, and the 1-D abundance functions using 2 hidden layers each with 10 nodes (Supplementary Information).”

Deep learning of intestinal epithelium metabolic topography

On page 17, we added the following sentences to specify the number of hidden layers and nodes in the neural network used for intestine data: “For the intestine, there are three relevant spatial dimensions: villus crypt-tip, epithelium apical-basolateral, and intestine proximal-distal (the latter potentially also covering any macroscopic patterns arising from imperfect sample processing or analysis). As such, we set K = 3.”
“We applied MET-MAP to the epithelial pixels to learn a metabolic depth function with two hidden layers of 120 nodes each, along with a linear abundance function (Supplementary Information). With visual assessment, one of the learned metabolic depths consistently captured the crypt-to-tip axis across all samples, validated by strong correlations with manually identified marker metabolites such as cholesterol sulfate and C20:3. In some samples, a second metabolic depth aligned with the brush border–to–basal membrane axis of epithelial cells, as indicated by strong correlations with metabolites such as linoleic acid. The third metabolic depth was typically associated with macroscopic spatial artifacts that varied between samples.”

On page 19, under **“Supervised porto-central axis construction”,** we specified the size of crops that were used in vein identification: “For each identified vein, a region of 12 × 12 pixels is cropped…”

6. “The authors mention that K=4 was used when the correct choice of K was unclear. However, it appears that K=4 was not used for any of the analyses. Instead, K=1 (line 588) was used for the analysis of the murine liver data, and K=3 (line 651) was used for the analysis of the murine intestine data. The authors then further refer to "one or two" significant metabolic depths that were identified depending on the individual sample quality and resolution (line 652-653). Presumably, these are the ones for which the corresponding weights of the depth functions were not "close-to-zero" In the spirit of my last comment, the authors should rephrase the text to clarify this and indicate the specific choices of K for each analysis they conducted.”

Thank you for catching this mistake. Absent expectations of particular spatial patterns, K = 1, 2, 3, or 4 is a reasonable starting point for initial testing of MET-MAP, but indeed all results in the paper use K = 1 for liver and K = 3 for intestine. This is now properly described in the revised manuscript.

7. “This is just a question out of interest to which I would appreciate an answer – there is no need to address this during the revisions: the authors introduce an adaptation of the GASTON model, which they refer to as MET-MAP. At a high level, the model takes the positional coordinates as input and predicts the abundance of different metabolites at the corresponding spatial locations. To achieve this, a one-hidden-layer neural network first outputs K scalars, referred to as metabolic depths, which are then input to a second neural

network. This second network may either include another hidden layer (for the liver) or consist of just a single layer (for the intestine) to predict the metabolite abundances. Given that the authors find almost all metabolites to show spatial gradients and many of them appear to be monotonically increasing or decreasing along the major metabolic axes, I am wondering if a non-linear PCA implemented by e.g. a simple autoencoder model could also provide similar estimates of those of the metabolic depth."

Response: This is a great question. Both an autoencoder neural network and the MET-MAP neural network have a similar structure containing: an encoder which maps the data to a lower dimensional latent space; a decoder which maps the latent space back to the data. In an autoencoder, both the input and the output layers are identical, and the encoder and decoder are inverse transformations.

Spatial MALDI data contains both metabolite abundances (features) and spatial coordinates for each feature. To directly apply an autoencoder to this data, one has to decide how to encode this data in input/output layers. One approach is to train the autoencoder only on the feature matrix (metabolite abundances). However, in this case the latent space will not represent any spatial correlations between features. The manuscript for the original GASTON method — on which MET-MAP builds — includes a comparison between PCA (linear dimensionality reduction) on features and the GASTON isodepth. For details, please see Supplement Information S10 in https://doi.org/10.1038/s41592-024-02503-3.
Alternatively, one could concatenate features (metabolite abundances) and spatial coordinates into a single input/output vector and train the autoencoder. In this case, the latent space will represent some potentially non-interpretable combination of features and spatial locations.

MET-MAP instead learns an interpretable spatial latent space (metabolic depth) by using an encoder on spatial coordinates followed by a decoder from the latent space to metabolite abundance. This architecture allows us to analyze the relationship between each metabolite and the learned spatial representation. Note that analogous encoder/decoder models have been used in computer vision where they are called neural fields or implicit neural representations. Because of these modeling differences, it is unclear how to directly compare the metabolic depth learned by MET-MAP to the latent spaces learned by an autoencoder.

To explore the capacity of PCA without attempting to build a spatial autoencoder, we ignored spatial position and simply carried out linear PCA on the pixel features (metabolite abundances). Plotting the principal component as an image provides a convenient way to interpret each PC spatially (see Figure below). PC1, which captures the largest variation in the dataset, changes spatially between blood vessels on the one hand and other liver tissue compartments on the other (including liver parenchyma and bile ducts), and does not capture portal-central gradients. Indeed, periportal and pericentral compounds show similar trends along PC1 (see Figure below). In contrast, PC2 recapitulates a portal-central pattern. By sorting compounds according to their PC2 loadings, periportal compounds show positive loadings and pericentral compounds negative loadings. Thus, an alternative way to analyze the data to find periportal and pericentral compounds is via PC2 loadings. A reassuring aspect to us is that all data analysis approaches yield to the same classification of compounds as periportal or pericentral. The advantage of MET-MAP is doing so in a way that automatically learns, from the spatial metabolomics, a smooth topographical map of the tissue.

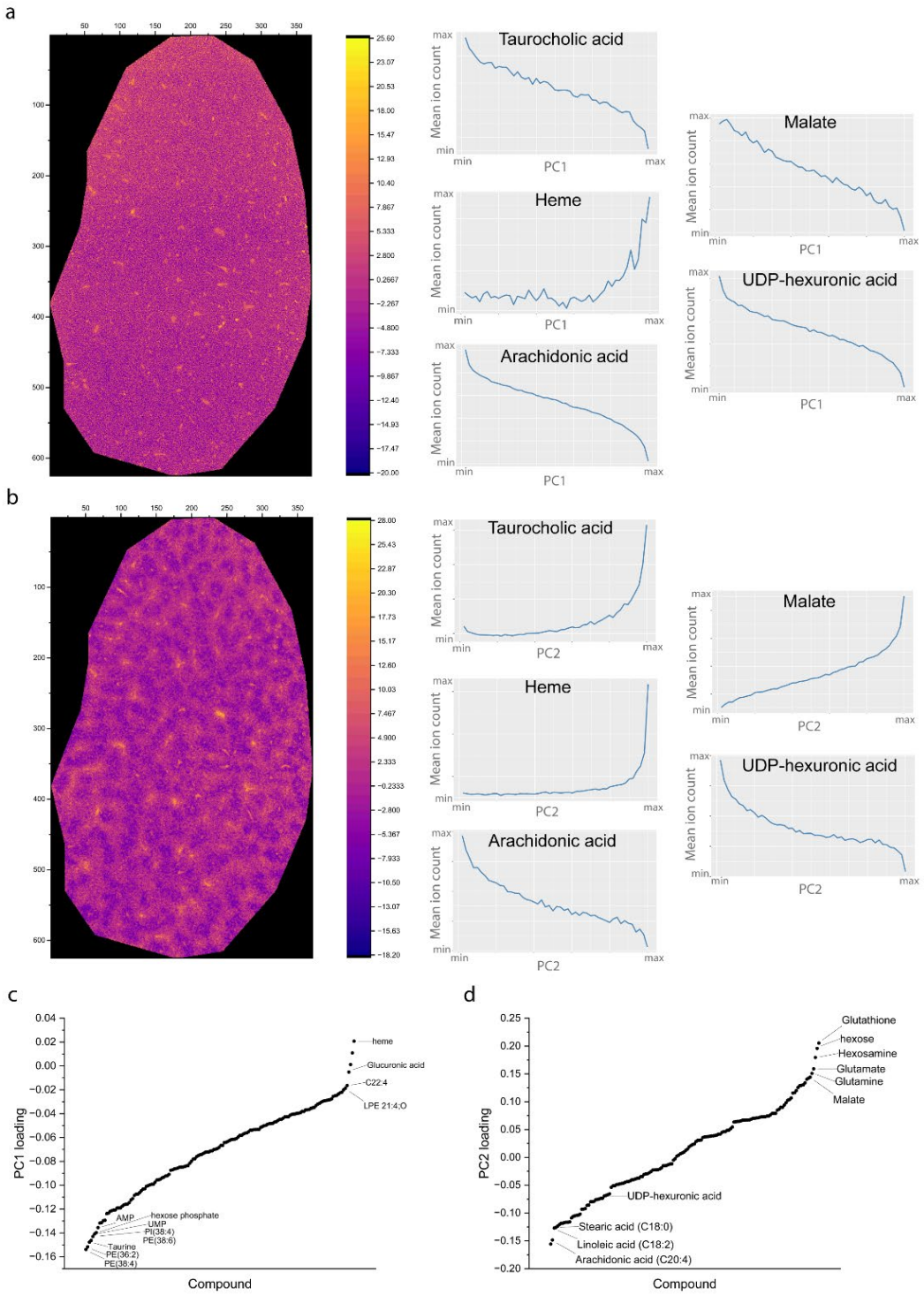

PCA of MALDI-IMS liver data. (a) Image of PC1 using MALDI data for one liver slice. Right panels show mean ion count as a function of PC1 for 5 compounds. Compounds showing opposite portal-central gradients show similar trends; thus, PC1 does not capture periportal-pericentral metabolism. (b) Same as (a) but for PC2. Trends on PC2 generally align with portal-central gradients, showing that PCA can capture relevant spatial metabolic information. (c), (d) Loadings for PC1 and PC2, respectively.

8. “Code for the MET-MAP Model (https://github.com/raphael-group/Multi-GASTON):
   The code itself is well-structured, easy to understand, and nicely commented. Unfortunately, the README file still seems incomplete, as the installation instructions, for example, are missing. Additionally, the file lacks a detailed description of how to reproduce the results of the study. However, given that the repository is intended as a resource for another Methods paper, I propose creating a separate GitHub repository that provides the minimal code required to reproduce the results of the study under review (see the last paragraph).”

We have created a new GitHub repository (https://github.com/raphael-group/MET-MAP). The repository contains the code for deep-learning analysis that was used in the paper and a tutorial to guide users how to use MET-MAP to reproduce the study results. The README file now describes how to install MET-MAP.

9. “Code for the supervised vein detection (https://github.com/xxing9703/Liver_vein_detection/tree/main):
   While the README file of this repository contains a high-level description of the main components of the implemented pipeline for identifying portal and central veins from MALDI images, it would significantly benefit from the following changes to enhance the usability of the code. First, the README is incomplete; for example, in the section describing the script “--script_get_imax.m”, the reference for where to download example images is missing. Second, the code itself should include docstring comments to consistently describe the input and output of the individual functions, as well as a few inline comments to improve its reusability. In this context, restructuring the code to group functions into larger modules and consolidating these into a single MATLAB file, instead of having separate files for each function, would also be beneficial.”

Response: We have created a capsule on Code Ocean that seamlessly runs the algorithm for supervised vein detection and portal-central axis construction. This allows the users to run the algorithm and easily reproduce the analysis results. We have included a detailed description of the algorithm in the capsule. Each function file in the capsule contains a comment header that describes inputs and outputs for each function. The capsule also contains raw liver spatial metabolomics “.csv” files that were used in the paper. Finally, we have consolidated all the functions of the code into a single MATLAB file “main.m”. The capsule has been submitted on Code Ocean so that reviewers can have access to the code.

We added the following sentence to the “**Supervised portal-central axis construction”** section in the **Methods** on page 19: **“**Readers can access the online Code Ocean capsule for supervised portal-central axis construction to facilitate analysis of the liver spatial metabolomics dataset.”

10. “Reproducing the study results:
    As mentioned before, the referenced repository used in the course of the study currently lacks sufficient details on how to reproduce the study results with the referenced data in https://doi.org/10.6084/m9.figshare.28049555.v3. Since the individual packages might be reused, or, in the case of Multi-Gaston, tailored towards more general use-cases, I recommend creating a new GitHub repository to outline how to reproduce the results of the

study by, among other things, using the repositories commented on above. I understand that this might be a time-consuming task, but it would greatly improve the reproducibility of the study and demonstrate how to apply the individual packages, thus promoting their reusability for other researchers in their own studies."

As mentioned above, we created a new GitHub repository to help reproduce the study results.

Referee #2:

General comment: “Samarah et al. used MALDI-based mass spectrometry imaging to assess metabolite localization in two organs from mice: liver and intestine. They develop a computational workflow to report metabolite gradients in both organs, focusing on periportal-pericentral gradients in the hepatic lobule, and crypt-tip gradients in the intestinal villus. They find that the great majority of detectable metabolites display localized gradients. Some of these gradients could be predicted from existing gene expression studies, but others (e.g. counterintuitive AMP/ATP gradients in the liver; F1P gradients in the liver after fructose feeding) identify interesting new aspects of nutrition and metabolism. The authors also use stable isotope-labeled nutrients to assess regional metabolic activity, and this adds another important dimension to this detailed characterization of metabolic localization within organs. I suggest that the paper be clarified or strengthened in a few areas.”

Response: We thank the reviewer for their feedback and suggestions to strengthen the paper.

1. “Given the untargeted nature of MSI, it is surprising that only 170 ions were “reliably detected.” I assume this means that these were reproducibly detected in independent samples, and molecular assignments could be made with high confidence based on standards? This seems to be what the Methods section implies, but this should be clarified in a sentence or two in the main text.”

Response: we agree with the reviewer’s comment that “170 ions” needs to be further clarified in the main text. We revised the number of compounds that we used in our analysis. For liver, we were able to detect across all samples 156 compounds consisting of metabolites and lipids that were assigned by at least accurate-mass match with the online databases HMDB and LIPID MAPS. For several compounds, we added MS/MS spectral match with either standards that were available to us or using online reference spectra (HMDB) as an orthogonal compound identification, and, when possible, validation by isotope tracing.

We made the following revision in the second paragraph on page 3 under the **Results** section “**Deep learning of liver metabolic topography**”: “From the raw data, 156 ions, including those corresponding to deprotonated and other forms (e.g., sodium, potassium and chloride adducts) of canonical lipids and water-soluble metabolites, were detected across independent mouse liver slices. Of these, 144 were deprotonated ions of canonical metabolites and lipids based on exact mass match and further identity confirmation (natural isotope abundance distribution, tandem mass spectrum, and/or isotope labeling; Supplementary Table 1).”

We also clarified our metabolite numbers in MALDI-IMS data processing section under Methods on page 15: “Since this process does not filter out background signal (including MALDI matrix peaks) and isotopologues, we matched m/z peaks with metabolites measured in-house by LC-MS analysis of liver and intestine extracts within a mass window of ± 15 ppm and with metabolites in the Human Metabolome Database (HMDB, https://hmdb.ca/) and lipids from LIPID MAPS (https://www.lipidmaps.org/), yielding 156 matching m/z peaks in liver and 206 in intestine. Of the 156 m/z peaks in liver, 144 corresponded to deprotonated metabolites and lipids (the remaining 12 peaks comprised other ion adducts, e.g., $[M+Na-2H]^-$, $[M+K-2H]^-$, or $[M+Cl]^-$) (Supplementary Table 1). For the intestine, 176 ions corresponded to deprotonated metabolites and lipids, with the remaining 30 peaks as sodium, potassium, chloride adducts or dehydrated ($[M-H2O-H]^-$) (Supplementary Table 3). Ion intensities for the 156 metabolites and lipids in liver and the total ion count at each pixel were extracted and used for deep-learning

analysis, whereas 206 metabolites and lipids were used for k-means clustering of the intestine data and subsequent analysis by MET-MAP.

2. "In Fig. 1f, how is the PN-to-CV normalized distance calculated? The absolute distance from portal to central varies among individual lobules, and likely with whether the slice through the lobule was axial or diagonal."

Response: In Fig. 1f, for a given pixel located on a portal-central axis, the position between the PN and CV is normalized 0 – 1 based on that axis' total distance, with 0 denoting PN and 1 CV. The normalization helps account for slice angle. Furthermore, we only studied axes of total distance 285 – 685 μm to avoid artifacts arising from incorrect assignment of the nearest PN or CV.

Revision: We added the following sentences to the Methods section under "**Supervised porto-central axis construction**" on page 19: "all portal and central veins are connected by straight lines under bond length constraints (285 ≤ L ≤ 685 um) to avoid joining central veins and portal nodes from distant lobules instead of the same one. To determine the position of a given pixel on a portal-central axis, the distance from the pixel to PN is normalized to the total distance between that PN and CV, with 0 denoting PN and 1 CV."

3. "In Fig. 2a, what are the "unclassified" metabolites? If these are unannotated masses, could their spatial correlation with other metabolites assist in identifying them?"

Response: Unclassified metabolites in Fig. 2a and Fig. 4a was used to refer to well-known compounds that do not fall neatly into the classification scheme used at the top of the figure (e.g. taurine is not a canonical amino acid, TCA intermediate, or the like). For clarity, we changed the label for these metabolites from "Unclassified" to "Other".

4. "In the isotope tracing experiments, did the authors acquire data on all isotopologues in the metabolites of interest? If so, this could add specificity and clarity to their interpretation of the labeling patterns. For example, it is surprising in the 13C-lactate infusions (Fig. 5b) that m+2 labeling seems to exceed m+3 labeling, at all locations, and that the m+3/m+2 labeling ratio is always far less than 1.0. This seems to argue against the notion that carbon entry via PC exceeds entry via PDH in the liver."

Response: We appreciate the reviewer's question and insightful comment. Yes, we did acquire data for all the detectable isotopologues (the MS analysis step is untargeted).

Regarding liver malate labeling form circulating [U-13C]lactate, we validated malate M+3/M+2 ratio in liver bulk measurement by LC-MS and found that, indeed, M+2 labeling exceeds M+3, as we observed in MALDI-IMS (M+3/M+2 = 0.6 in bulk liver) (See Figure below). Thus, the MALDI measurements align with bulk metabolomics.

What is the meaning of the malate M+3/M+2 ratio? In addition to coming from lactate/pyruvate via PDH, malate M+2 is also generated from PC-derived M+3 oxaloacetate upon TCA-cycle turning. The greater M+2 relative to M+3 malate from lactate accordingly requires TCA turning but not PDH flux.

A complementary way to assess PC and PDH flux is by infusing [1-13C]lactate which only labels malate via PC, as the label is lost upon either TCA turning or passage through PDH. We carried out new experiments infusing [1-13C]lactate and measuring spatial gradients in malate

labeling. Consistent with the [U-13C]lactate tracing, we observed higher periportal than pericentral malate (M+1) fraction, confirming higher periportal PC activity (Extended Data Figure 7, also shown below). Thus, we observe consistent liver TCA labeling between MALDI imaging mass spectrometry and bulk LC-MS, and consistent spatial labeling patterns with 2 different tracers of pyruvate carboxylase activity.

We updated the text in the manuscript, page 7, second paragraph under “Substrates driving spatial TCA metabolic gradients”: “In contrast, pyruvate carboxylation to oxaloacetate generates M+3 TCA intermediates. These can either feed gluconeogenesis or be converted into M+2 TCA intermediates by TCA turning (Fig. 5d). Thus, the malate M+3/M+2 ratio reflects pyruvate carboxylase flux relative to TCA turning. Consistent with gluconeogenesis being periportal, the malate M+3/M+2 ratio was greater periportally (Fig. 5f). Tracing with [1-13C]lactate, which selectively labels malate made via pyruvate carboxylase, further supported periportal localization of pyruvate carboxylase activity (Extended Data Figure 7).”

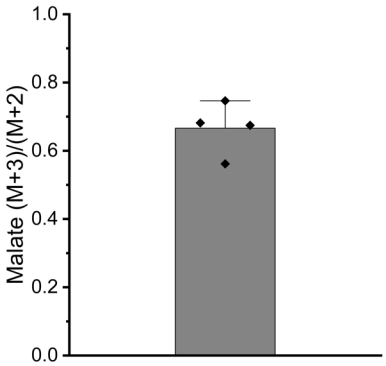

Bulk liver malate M+3/M+2 ratio from mice infused with [U-13C]lactate (n = 4).

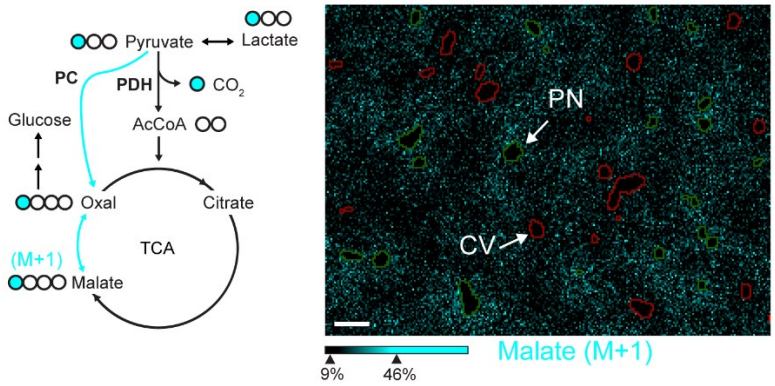

Extended Data Figure 7. Higher periportal pyruvate carboxylase activity. Left panel, schematic of malate M+1 labeling from circulating [1-13C]lactate in liver through pyruvate carboxylase (PC) (cyan arrows). Colored circles 13C; white circles 12C. Right panel, MALDI image of malate M+1 in liver after correction for natural isotope abundance from mouse infused with [1-13C]lactate. Scale bar = 300 μm.

5. “The authors nicely show that lactate contributes more to glutamate in well-oxygenated crypts, and glutamine is a more meaningful carbon source in the tips. This implies that different carbon sources are catabolized differently along the villus. But I am still confused as to why citrate is more abundant in the crypts, while other TCA cycle intermediates are relatively depleted. Is there a change in aconitase/IDH expression between crypt and tip?”

Response: We thank the reviewer for the important question. Yes, aconitase and isocitrate dehydrogenase 3a, the key enzymes for citrate catabolism, localize to the tips (DOI: 10.1038/s42255-021-00504-6). This has been added to the manuscript. In light of this data, there are 2 complementary reasons for the crypt localization of citrate: (i) the key citrate catabolizing enzymes are tip localized and (ii) malate to citrate flux is greater in crypts due to better oxygen supply and associated greater capacity for malate → oxaloacetate → citrate conversion enabled in part by lactate → acetyl CoA → citrate → KG/glu, which is clearly up in the crypts by isotope tracing.

We added aconitase and IDH3a localization in the second paragraph under “**Spatial discordance in TCA and energy metabolites along crypt-villus axis”** on page 6: “In contrast, aconitase and isocitrate dehydrogenase 3a, which consume mitochondrial citrate and promote its conversion into downstream TCA intermediates like malate, localize to tips[5,22] (Extended Data Fig. 8a). Their spatial pattern may contribute to citrate and malate localizing in opposing ends of intestinal villi.”

6. “In Fig. 2a, consider changing the color scheme to make it easier to differentiate the pentose phosphate pathway intermediates (accumulated in periportal region) from the phospholipids (accumulated in the pericentral region).”

Thank you for the suggestion. We have done so.

Referee #3:

General comment: “In this work, Samarah et al perform comprehensive spatial metabolomics of the major metabolic organs – the small intestine and the liver, in mice. These tissues are highly structured and exhibit strong gradients of oxygen, nutrients and morphogens. As a result, both mRNA and protein levels for most genes have been shown to strongly vary along the axes of the repeating units of these tissues, lobules in the liver and crypt-villi units in the intestine. However, obtaining high-spatial resolution spatial maps of the metabolites has been challenging, in part due to the lower sensitivity of spatial approaches for measuring metabolites, such as MALDI. The authors overcome this limitation with a sophisticated AI-driven approach that enables annotating individual pixels to the major tissue coordinates. They then pool many pixels from similar zones, thus increasing signal to noise ratio and sensitivity, yielding a highly detailed map of more than a hundred metabolites. They use the results to obtain interesting insights regarding energy and metabolite utilization. Importantly, they perform the mapping on both a fasted ‘steady state’, as well as after refeeding fasted mice with labeled fructose and glucose, enabling spatial mapping of the metabolic fluxes associated with the absorption of these central nutrients. The paper is both an important resource and a methodological breakthrough, since the approaches presented can be readily generalized to enable attaining similar spatial metabolic maps in other structured tissues, as well as in tumors.”

Response: We thank the reviewer for the supportive feedback. We agree that our work provides a resource of metabolic zonation data in the liver and small intestine and a pipeline that will be transferable also to other biological tissues.

1. “Some metabolites are labile, and their measurements could potentially be skewed by factors such as temporal delays in tissue processing for MALDI, as well as by features of the technique, such as matrix effects. The study focuses on relative changes along the axes of the tissues, so such effects may be less critical, however, it would strengthen the paper to add a controlled measurement using an orthogonal approach. For example, LC-MS bulk measurements of several metabolites, demonstrating the relative proportions between them are quantitatively similar to those observed with the MALDI measurements.”

Response: We thank the reviewer for the suggestion. We analyzed liver slices by MALDI and liver extracts by LC-MS and compared signals. For MALDI, we used the mean ion count across all pixels in each liver slice. Across the two methods, signals were correlated (Pearson’s r = 0.6, $p = 1.52 \times 10^{-8}$) (Extended Data Figure 1a, also shown below).

The outliers are informative. Cyclic AMP is disproportionately higher in MALDI and may come from in-source fragmentation of NADH. In-source fragments are found also in LC-MS but we exclude them based on chromatographic separation, whose absence is a limitation of MALDI. Uric acid is also higher in MALDI, but in this case MALDI seems to be the more biologically informative technique, with the difference reflecting higher sensitivity for MALDI as evidenced by substantially lower LOD for uric acid standard by MALDI-MS compared to LC-MS (Extended Data Figure 1b, shown below). Taurodeoxycholic acid signal is lower in MALDI. Its signal is strongly spatially localized. Averaging across pixels may underestimate the absolute quantity in this case. Palmitate is also lower in MALDI, representing a second case where MALDI seems to be preferred, as palmitate is common environmental contaminant in LC-MS.

We added the correlation between MALDI-IMS and LC-MS in the main text (first paragraph of the Results section): “Across metabolites, MALDI-IMS signals correlated with bulk metabolomics (Extended Data Figure 1).”

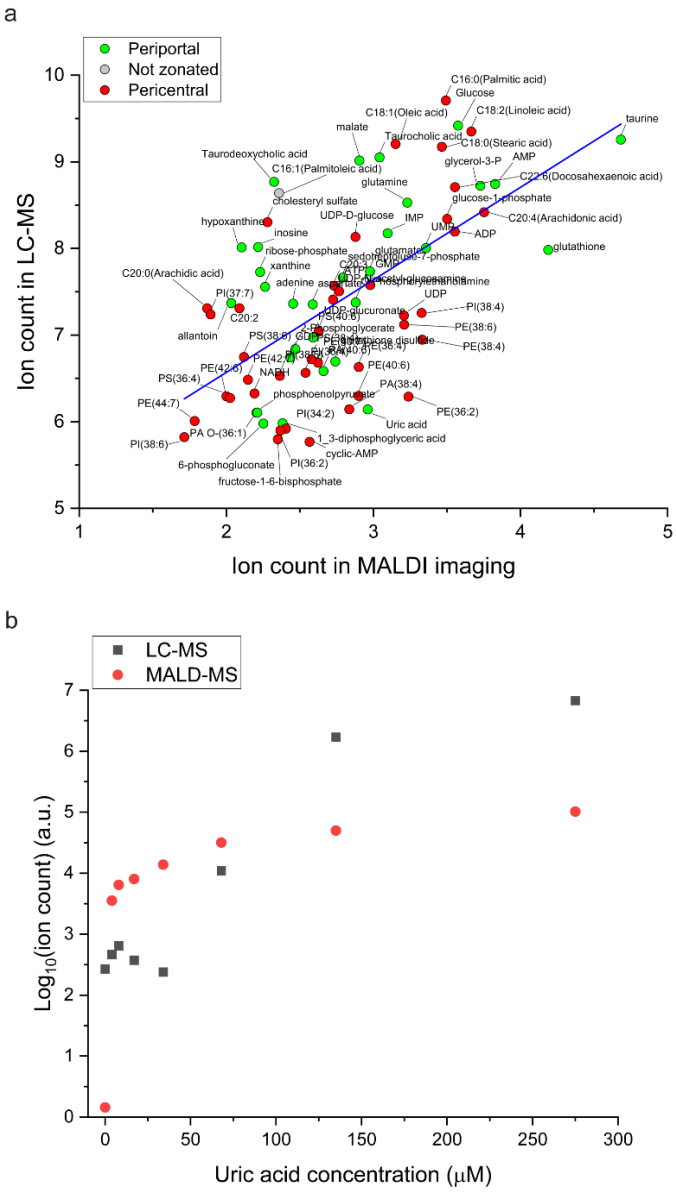

Extended Data Figure 1. Metabolite counts correlate in MALDI imaging and bulk metabolomics. (a) Correlation between ion counts (log10 scale) in LC-MS of bulk liver (n = 11) and MALDI-IMS of liver tissue slice (n = 7). (b) Uric acid (disproportionately higher in MALDI-IMS) standard analysis by LC-MS and MALDI-MS.

2. “Line 175-176 – Liver energetic demands are also high because of protein translation. The periportal zone is the main site of translation of secreted proteins (such as albumin, complement and clotting factors), I would mention this task as well.”

Response: Great point. We have done so (page 5, second paragraph).

3. “Line 221 – Cholesterol absorption from the lumen is strongly zonated towards the villus tip (e.g. both the mRNA and proteins of NPC1L1, https://www.cell.com/cell/fulltext/S0092-8674(18)31164-4 and Harnik et al.). Might this also contribute to the tip zonation of Cholesterol sulfate?”

Response: We appreciate the reviewer’s valuable insight. It is possible that our observation of strong cholesterol sulfate zonation in the villus tips is linked to zonation of cholesterol transport. Furthermore, the sulfotransferase SULT2B1, which catalyzes the sulfonation of cholesterol, is also strongly zonated towards the villus tips. A previous study has shown that reduction in expression of the gene Sult2b1 in mice results in substantial loss of cholesterol sulfate (Morino et al., 2023, https://doi.org/10.3389/fimmu.2023.1131146). Thus, we also attribute localization of cholesterol sulfate in the villus tips to a combination of cholesterol uptake and cholesterol sulfonation enzyme localization.

We added the following sentence to page 6, line 229: “This localization also follows the cholesterol transporter, NPC1L1, and the cholesterol-sulfonation enzyme, SULF2B1, both of which are strongly localized towards the tips[22,53].”

4. “One of the most prominent zonated programs at the mouse villus tip is the expression of the purine metabolism enzymes Enpp3, Nt5e (CD73), Slc28a2 and Ada, which convert ATP (presumably from luminal bacteria) to AMP, then to Adenosine and finally to inosine (https://www.cell.com/cell/fulltext/S0092-8674(18)31164-4). Can this program in tip enterocytes affect some of the observed gradients in ATP and AMP?”

Response: We thank the reviewer for the valuable insight. To examine whether the referenced purine metabolism program mentioned above contributes to the observed AMP and ATP gradients along the crypt-villus axis, better detection of downstream catabolites of AMP, particularly, adenosine and inosine, is needed (these metabolites are in the list of 156 quantified ions in liver but are unfortunately not quantified in the intestine). We have been continuously working on improving detection of these nucleosides but do not have adequate intestinal signal yet.

5. “KHK protein peaks at the middle of the villus rather than at the villus tip as mentioned in EDF6f caption. It is different than most transporters and nutrient-processing enzymes, the protein expression of which peaks at the villus tip. This could potentially explain the stronger absorption the authors measure for fructose at the mid/bottom villus shortly after the gavage. I would change the legend of EDF6f to reflect the mid-villus localization of KHK.”

We thank the reviewer for the insightful comment and have updated the manuscript accordingly.

6. “One of the riddles in liver biology is the glucose paradox (Katz and McGarry, 1984), positing that the main substrate of glycogen synthesis in the liver after a meal is lactate, via the indirect pathway, rather than glucose. Moreover, it was postulated that this indirect lactate utilization is specifically applied in the portal zones (Figure 3 in doi: 10.1146/annurev.nu.16.070196.001143). Can the results of the labeled fructose+glucose

refeeding experiment be used to assess this potential differential usage of lactate vs. glucose as a substrate for glycogen replenishment postprandially?"

Response: We thank the reviewer for the interesting question. Based on our results in Extended Data Figure 9, the contribution of oral glucose (based on ^{2}H labeling) to liver glycogen (as inferred from UDP-glucose labeling) is preferentially higher in the pericentral zone. In contrast, circulating lactate feeds periportal UDP-glucose. Together, these results align with the notion that liver zonation of glycogen synthesis is substrate dependent, with glucose feeding pericentral glycogen synthesis and lactate periportal.

We added the following sentence in page 8 to refer the reader to the dependence of glycogen-synthesis zonation on the substrate: "Prior research suggested that lactate might preferentially feed periportal glycogen synthesis[15], and we confirmed this to be the case (Extended Data Fig. 9)."

7. "Line 556 – MALDI-IMS data processing – Should the MALDI signal be normalized to the summed signal of all measured metabolites before averaging over pixels of same zone to obtain the zonation profiles? If different pixels have different total metabolite yield (metabolite capture rates), such normalization could potentially control for this extrinsic source of variability."

We thank the reviewer for the important question. The reviewer is correct that this is a beneficial normalization. Indeed, this is exactly what was done: Before training the MET-MAP neural network to solve for metabolic depth, raw metabolite abundance at each pixel was normalized to the pixel TIC. We mentioned this in the Methods section under "**Deep learning of liver metabolic topography**": "Before training the neural network to solve for metabolic depth d, raw metabolite abundance $[a_{i,m}] \in R^{N \times M}$ was first normalized using Total Ion Count (TIC) at individual pixels and log-transformed." The same was done for intestinal epithelium data.